doi.org/10.1002/hlca.202300170

RESEARCH ARTICLE

HELVETICA chimica acta

Improved Synthesis of Chiral 1,4,7-Triazacyclononane Derivatives and Their Application in Ni-Catalyzed Csp^3–Csp^3 Kumada Cross-Coupling

Chi-Herng Hu,[a] Ju Byeong Chae,[a] and Liviu M. Mirica*[a]

[a] Department of Chemistry, University of Illinois at Urbana-Champaign, 600 S. Mathews Avenue, Urbana, Illinois 61801, United States, e-mail: mirica@illinois.edu

Dedicated to *Scott E. Denmark* on the occasion of his 70th birthday and award of the Paracelsus prize

Herein, we report four new chiral 1,4,7-triazacyclononane (TACN) derivatives and their corresponding nickel(II) chloride complexes. All TACN ligands are bearing one chiral N-substituent and two alkyl (methyl or *tert*-butyl) N-substituents, and we have developed a new synthetic method for the dimethyl-substituted TACN derivative, in order to prevent the rotational isomers that hinder the cyclization reaction. The nickel complexes change their coordination geometry significantly depending on the steric bulk of the N-alkyl substituents, from a dinuclear tris(μ-chloro)dinickel complex to mononuclear Ni-dichloride and Ni-chloride complexes. These complexes were then employed in the alkyl-alkyl Kumada cross-coupling reaction and revealed that the more sterically hindered ligands produced more homocoupled product rather than the cross-coupled product, while the mononuclear Ni-dichloride complex exhibited significantly lower catalytic activity. These chiral complexes were also employed in enantioconvergent cross-coupling reactions as well, to afford significant enantioenrichment. Overall, the least sterically hindered Ni complex yields the best yields in the alkyl-alkyl Kumada cross-coupling reaction among the four complexes investigated, as well as the highest enantioselectivity.

Keywords: 1,4,7-triazacyclononane, chiral ligands, cross-coupling, nickel, nickel complexes, Kumada cross-coupling reaction.

Introduction

1,4,7-Triazacyclononane (TACN) macrocycles are strong tridentate metal chelators that have been employed in various applications of inorganic chemistry, such as low-temperature bleaching,[1] bioimaging,[2–8] and small-molecule activation.[9–12] The cyclic 9-membered ring of TACN enforces a facial binding motif when interacting with metal ions that adopt an octahedral geometry,[13] and thus leaving three open coordination sites that are oriented *cis* to each other.

Even though the synthesis of Ts_2HTACN was reported back in 1937 by reaction of bis(2-chloroethyl)ethylenediamine ditosylate and ammonia,[14] the synthesis of the simplest TACN, H_3TACN, was first reported by Koyama and Yoshino in 1972 through the detosylation of Ts_2HTACN in the presence of 30% hydrobromic acid in acetic acid.[15] In more modern methods, the TACN macrocyclic ring is constructed through macrocyclization of diethylene triamine tritosylate and ethyleneglycol ditosylate in the presence of cesium carbonate,[16,17] and complete detosylation of Ts_3TACN in concentrated sulfuric acid generates H_3TACN (*Scheme 1*). Alkylation of H_3TACN produced R_3TACN (R = Me, ^{i}Pr, or other alkyl groups) with various steric bulk. On the other hand, asymmetric TACN could be synthesized by selective detosylation of Ts_3TACN, to afford the Ts_2HTACN or TsH_2TACN intermediates needed for further derivatization.

Supporting information for this article is available on the WWW under https://doi.org/10.1002/hlca.202300170

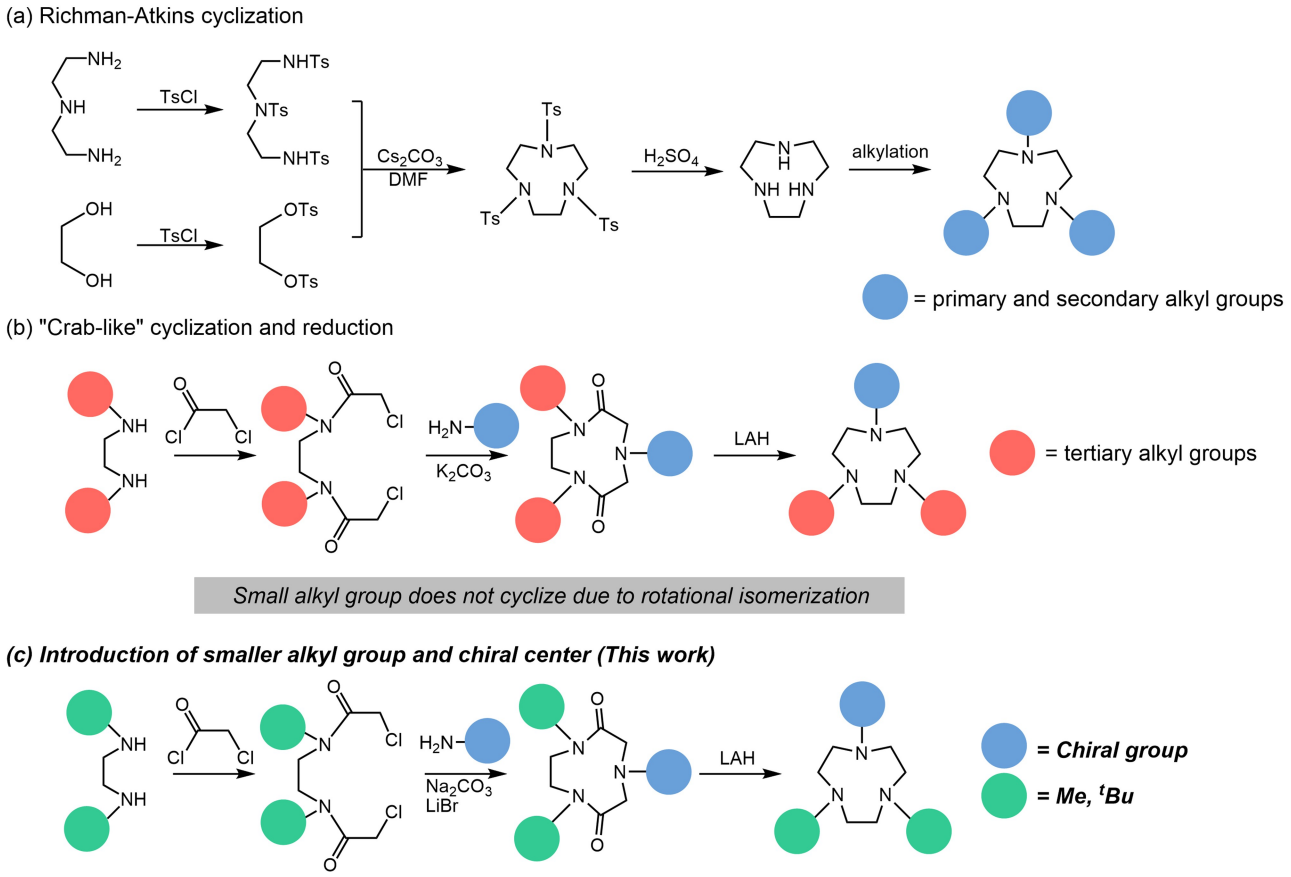

Scheme 1. Synthesis of TACN derivatives by different synthetic methods. (a) Richman-Atkins cyclization. (b) 'Crab-like' cyclization and reduction. (c) This work: introduction of small alkyl N-substituents and a chiral N-substituent.

Alternatively, the 9-membered ring could be formed through the reaction of bis(chloroacetyl)ethylenediamine and primary amine. Since 2013, Scarborough and coworkers have synthesized numerous TACNs through this 'crab-like' route with tertiary and chiral amine substituents previously inaccessible with the classical cyclization method.[18,19] Nevertheless, the method tends to be ineffective when the bis(chloroacetyl)ethylenediamine bears less bulky substituents, such as methyl or isopropyl, due to rotational isomers. To date, only few asymmetric TACNs have been reported with one stereocenter.[19,20] Moreover, previous reports mainly focused on synthetic development of the TACN derivatives, and the reactivity of corresponding metal complexes was not investigated in detail.

Recently, our group has reported the use of $^{i}Pr_3$TACN in Ni-catalyzed Kumada cross-coupling reactions.[21,22] This led us to explore the C–C bond forming reactivity of chiral TACNs which could potentially lead to asymmetric cross-coupling reactions induced by the chiral N-substituent. Herein, we describe the preparation of four new chiral TACN derivatives bearing one stereocenter, (*S*)-1,4-dimethyl-7-(1-phenylethyl)-1,4,7-triazonane (**3a**), (*R*)-1-(3,3-dimethylbutan-2-yl)-4,7-dimethyl-1,4,7-triazonane (**3b**), (*S*)-1,4-di-*tert*-butyl-7-(1-phenylethyl)-1,4,7-triazonane (**6a**), and (*R*)-1,4-di-*tert*-butyl-7-(3,3-dimethylbutan-2-yl)-1,4,7-triazonane (**6b**). The corresponding nickel complexes were synthesized and characterized (see below). The increment of the steric bulk of the alkyl groups significantly changes the geometry of the corresponding Ni complexes from a dinuclear tris(μ-chloro)dinickel complex to mononuclear Ni-dichloride and Ni-chloride complexes. Also, we have found that the least sterically hindered Ni complex yields the best yields in the alkyl-alkyl Kumada cross-coupling reaction among the four complexes investigated.

Results and Discussion

Synthesis of New TACN Derivatives Bearing One Chiral Stereocenter

In 2018, Scarborough and coworkers reported a systematic study on the preparation of TACN ligands with two N-^{t}Bu substituents and a third bulky N-substituent through the crab-like route.[19] Nevertheless, while RMe_2TACN ligands have been reported previously,[23,24] such TACN ligands with two N-methyl substituents could not be obtained using the crab-like route reported in 2018. Previous literature has implied that the use of LiBr is essential, likely because the lithium cation imposes a templating effect where the precursor favors an intramolecular S_N2 cyclization instead of intermolecular substitution reactions.[25] Therefore, we set out to prepare RMe_2TACN using LiBr as an additive. Gratifyingly, the dimethyl bischloroacetamide (**1**) reacted with (*S*)-1-phenylethan-1-amine (PhEt–NH_2) to produce the desired macrocycle (*Scheme 2*). However, ESI-MS spectrum of the reaction mixture indicated the formation of a wide distribution of side products, including the uncyclized intermediate, overaminated product, an 18-membered macrocycle, and uncyclized oligomeric products (*Scheme 3*). The similar polarity of these byproducts caused difficulty in purification of the crude material, and a combination of a silica plug and recrystallization was required to obtain a higher quality material for the next step. Reduction of the TACN-dione with $LiAlH_4$ generates **3a**, which is purified by vacuum distillation. Compound **3b** was prepared following the same procedure, using (*R*)-3,3-dimethylbutan-2-amine (MeNp–NH_2) as the chiral amine. The R^tBu_2TACN ligands, on the other hand, were synthesized using the reported optimized procedure. The reaction of di-*tert*-butyl bischloroacetamide **4** with either one of the chiral amines produced the cyclized products in high yields, and reduction with $LiAlH_4$ generates the desired ligands **6a**/**6b**. The chirality of ligands is confirmed to be enantiomerically pure by chiral gas chromatogra-

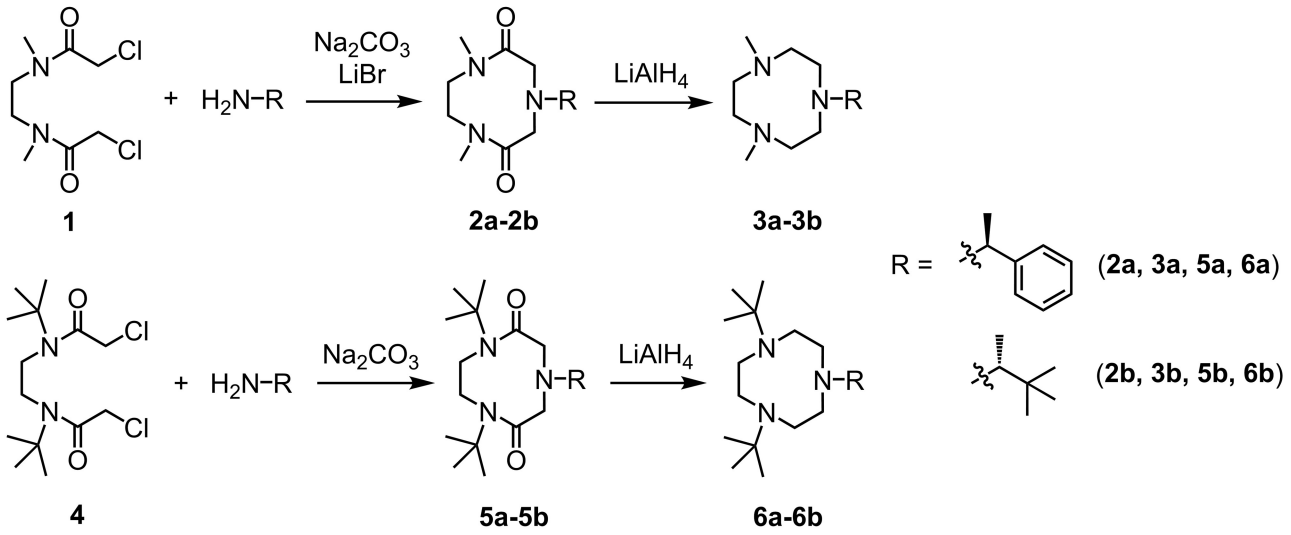

Scheme 2. Synthesis of TACN derivatives **3a**, **3b**, **6a**, and **6b**.

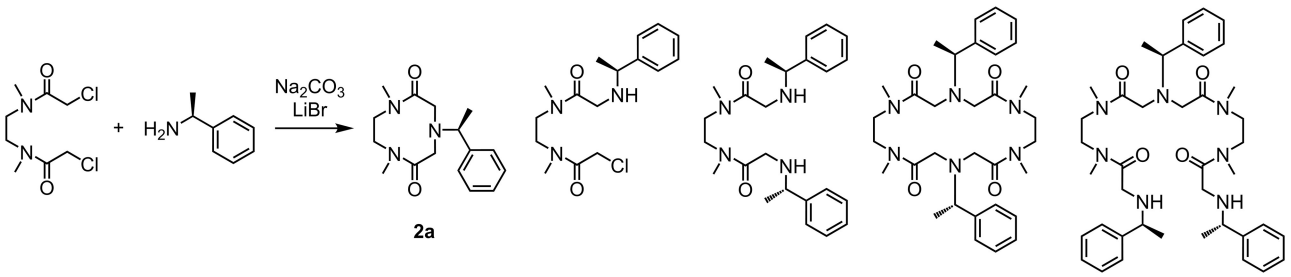

Scheme 3. Synthesis of cyclized TACN-dione precursor and the side products observed by ESI-MS.

phy, indicating that the corresponding Ni complexes are pure enantiomeric species as well.

Synthesis and Characterization of Ni Complexes

The reaction of the four new chiral TACN ligands with $NiCl_2$(DME) yields a series of mononuclear and dinuclear nickel complexes depending upon the steric bulk of the ligand (*Scheme 4*). When **3a** was added to $NiCl_2$(DME), an immediate color change occurred, however, no crystals could be obtained despite numerous trials. Since a sandwich-type dinuclear structure with three bridging halides has been observed for Me_3TACN,[26] we hypothesized that the excess chloride anion is competing with amine coordination. Therefore, 0.5 equiv. KPF_6 was added to remove the chloride by precipitation of KCl. Indeed, we were able to purify and crystallize a teal solid as a dinuclear nickel complex with hexafluorophosphate as the counteranion, **7**, which is a dinuclear Ni complex with three bridging chloride ions, $[(\mathbf{3a})_2Ni_2(\mu\text{-}Cl)_3)](PF_6)$, and each Ni center has a distorted octahedral geometry with an elongated axial Ni–N bond. The chiral phenylethyl (PhEt) groups face the same direction, while the methyl groups are pointing in the opposite side. The Ni–Ni distance is 3.086 Å, which is longer than the 3.043 Å distance in $[(Me_3TACN)_2Ni_2(\mu\text{-}Cl)_3]$,[26] indicating that bulkier PhEt groups elongate the Ni–Ni distance. In contrast, the reaction of **3b** and $NiCl_2$(DME) generates a green 5-coordinate square pyramidal mononuclear nickel-dichloride complex $[(\mathbf{3b})NiCl_2]$, **8** (*Scheme 4*). As the methylneopentyl (MeNp) group is bulkier than the PhEt group, it may prevent dimerization of two Ni centers. Moreover, the Ni–Cl bond that is closer to the N–MeNp substituent is longer than the other Ni–Cl bond ~0.08 Å, likely due to a steric clash (*Figure 1*). For **6a** and **6b**, the sterically demanding *tert*-butyl groups further limit the coordination number, and 4-coordinate nickel monochloride complexes $[(L)NiCl](PF_6)$ (L = **6a** or **6b**) were afforded in the presence of 1 equiv. KPF_6. This coordination is consistent with the previously reported $[(^tBu_3TACN)NiBr](PF_6)$ complex,[18] suggesting that having two *tert*-butyl groups is bulky enough to make the complex adopt a 4-coordinate geometry. Notably, in complex **10** the ^{t}Bu group of the N–MeNp substituent points away from the Ni center, likely due to the two bulky N-*tert*-butyl groups.

Kumada Cross-Coupling Reactivity Studies

With these complexes in hand, we investigated their reactivity to probe the role of the coordination environment and steric hindrance of the TACN ligands

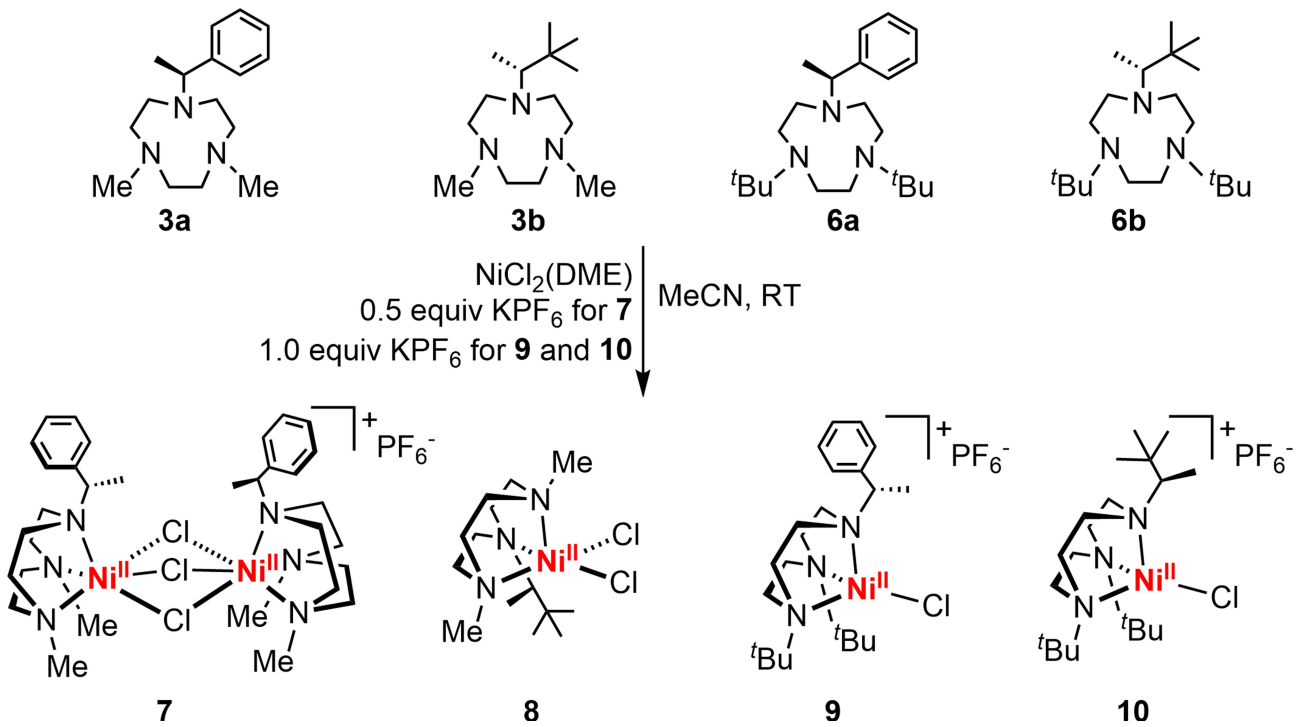

Scheme 4. Synthesis of chiral nickel-chloride complexes **7**–**10**.

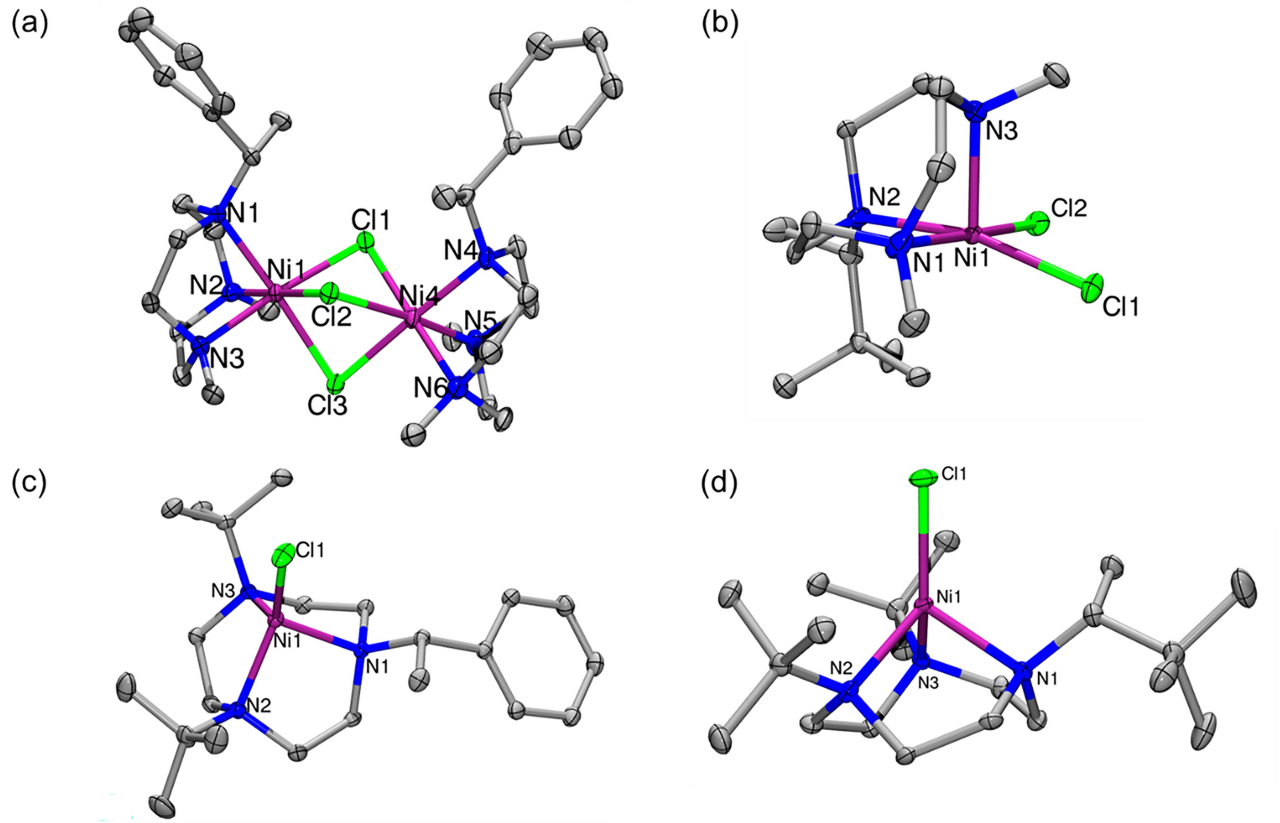

Figure 1. ORTEP representations (50% probability ellipsoids) of solid-state structures of Ni complexes a) cation of **7**, b) **8**, c) cation of **9**, and d) cation of **10**, (hydrogen atoms and counteranions omitted for clarity).

on their catalytic properties (*Table 1*). Since nickel complexes are commonly employed in Kumada cross-coupling reactions, we performed the Kumada cross-coupling reaction with an alkyl halide and an alkyl Grignard. We chose the longer alkyl halide and Grignard reagents *n*-heptyl iodide and *n*-octyl magnesium chloride to track all possible products generated during the reaction. In a previous study we found that the addition of MeCN helps to improve the product formation and we were able to optimize the reaction conditions.[22] Under the optimized conditions, the highest yield (35%) was obtained when **7** was employed as the catalyst from the four complexes, likely due to the least sterically hindered ligand environment. By comparison, **8** generated the least amount of the C–C coupled product (8%), with a large amount of unreacted alkyl halide being observed (*Table S1*). This might be attributed to the steric bulk of the N–MeNp group which might prevent the binding of MeCN to the Ni center, in order to stabilize a Ni(I) intermediate and also to facilitate reductive elimination.[22] For **9**, a 29% yield of cross-coupled product was obtained, yet more homocoupled alkyl halide (tetradecane) and the β-hydride eliminated product octene were obtained, suggesting that the two N-^{t}Bu substituents may enforce a geometry at the

Table 1. Catalytic Kumada cross-coupling reactions.

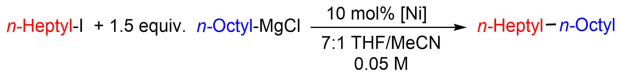

Entry	Ni Complex[a]	Yield [%][b]
1	without Ni catalyst	0
2[c]	**7**	35
3	**8**	8
4	**9**	29
5	**10**	21

[a] Standard conditions: *n*-heptyl iodide (0.1 mmol, 1.0 equiv.), Ni complex (10 mol%), MeCN (0.25 mL, 50 equiv.), *n*-octylMgCl (0.15 mmol, 1.5 equiv.), 1.25 mL THF, 2 h, RT. [b] Yields were obtained by GC-FID and were corrected using calibration curves, using dodecane as an internal standard, and represent average values of at least three independent measurements. [c] 5 mol% of catalyst is employed for the dinuclear complex **7**.

Ni center that prevents transmetalation and promotes β-hydride elimination more readily. Finally, complex **10**, containing the TACN ligand with both the N–MeNp substituent and two *tert*-butyl groups, generates the cross-coupled product in a 21% yield, a value between those obtained for **8** and **9**, along with a significant amount of unreacted alkyl halide being left and β-hydride eliminated products being generated. Overall, these results show that having sterically hindered TACN ligands significantly inhibits the Ni-catalyzed Kumada cross-coupling reaction and leads to side product formation. Next, we investigated enantioselectivity of the complexes using secondary alkyl halide, (±)2-iodobutane (*Table 2*, and *Figures S22–S24*). When we employed precatalysts **7**, **9**, and **10** except for **8** which showed the lowest product yield, we were able to obtain enantiomeric excess (*ee*) of 70%, 58%, and 34%, respectively. The low *ee* might be because the chiral group is far from the Ni center, less affecting to the enantioselectivity. Especially having two bulky *tert*-butyl groups instead of two methyl groups significantly decreased *ee* (70% to 58%), further supporting that more accessible chiral group to the Ni center is necessary to get higher *ee*.

Conclusions

In summary, we report four new chiral 1,4,7-triazacyclononane (TACN) derivatives and their corresponding nickel(II) chloride complexes. The synthesis of the *N*,*N*′-dimethyl TACN ligands having one chiral N-substituent was achieved with LiBr as an additive, which likely prevents the formation of rotational isomers. Moreover, the nickel complexes showed significant changes of their coordination geometry depending on their ligand environment, from a dinuclear tris(μ-chloro)dinickel complex to mononuclear Ni-dichloride and Ni-chloride complexes. These complexes were employed as catalysts in alkyl-alkyl Kumada cross-coupling reactions, and it was found that the complexes with bulkier ligands inhibit cross-coupled product formation, homocoupled or β-hydride eliminated products being formed instead. Overall, we have found that the least sterically hindered Ni complex yields the best yields in the alkyl-alkyl Kumada cross-coupling reaction among the four complexes investigated as well as the highest enantioselectivity, and thus one has to carefully consider the bulkiness of the tridentate N-donor ligands when employing them in Ni-mediated cross-coupling reactions.

Table 2. Enantioconvergent cross-couplings of unactivated alkyl electrophiles.

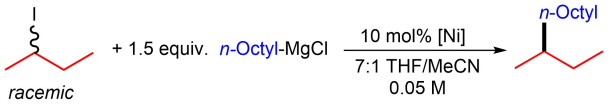

Entry	Ni Complex[a]	ee [%][b]	Yield [%][c]
1	**7**	70	13
2	**9**	58	21
3	**10**	34	8

[a] Standard conditions: 2-iodobutane (0.1 mmol, 1.0 equiv.), Ni complex (10 mol%), MeCN (0.25 mL, 50 equiv.), *n*-octylMgCl (0.15 mmol, 1.5 equiv.), 1.25 mL THF, 2 h, RT. [b] ee was determined by chiral GC-FID analysis. [c] Yields were obtained by GC-FID and were corrected using calibration curves, using dodecane as an internal standard, and represent average values of at least three independent measurements.

Experimental Section

General Experimental Details

All reactions were performed in ambient conditions unless otherwise stated. Solvents were purified prior to use by passing through a column of activated alumina using an MBraun solvent purification system. All starting materials and reagents, unless otherwise specified, were obtained from commercial sources and used without further purification. The bischloroacetamides[19] were synthesized following literature procedures. ^{1}H- and ^{13}C-NMR spectra were recorded using a Bruker 400 MHz or 500 MHz spectrometer. GC-MS data was collected using an Agilent 7890B GC Series System and an Agilent 5977B Mass Selective Detector. GC yields [%] were determined by GC-FID with a calibration curve vs. dodecane as an internal standard. Chiral gas chromatographic (GC) analysis was performed on an Agilent 6890 N Series instrument equipped with FID detectors using a J&W Cyclosil-B column. Electrospray ionization mass spectrometry (ESI-MS) was recorded on a Water Q-TOF Ultima ESI instrument by the Mass Spectrometry Laboratory at the University of Illinois at Urbana–Champaign (UIUC).

Elemental analysis was carried out by the Microanalysis Laboratory at UIUC using an Exeter Analytical - Model CE440 CHN Analyzer. The boiling point was measured using a thermometer during vacuum distillation with a short-path condenser.

1,4-Dimethyl-7-[(1*S*)-1-phenylethyl]-1,4,7-triazononane (**3a**). An oven-dried 1 L round bottom flask under N_2 was charged with LiBr (5.76 g, 2.0 equiv.), Na_2CO_3 (28.00 g, 8.0 equiv.), and bischloroacetamide **1** (8.00 g, 1.0 equiv.) in anhydrous acetonitrile (500 mL). The mixture was heated to reflux and PhEt–NH_2 (4.7 mL, 1.1 equiv.) was added in one portion. After gentle reflux over **3d**, the mixture was cooled to 0 °C in ice bath, and the white solids were filtered off. The solution was concentrated under reduced pressure to a pale-yellow oil and redissolved in dichloromethane (40 mL). The dichloromethane solution was washed with deionized water, dried over $MgSO_4$, passed through a silica plug, and concentrated to an oil. Diethyl ether was added to triturate the desired product, and the solid was collected by filtration to afford **2a** as an off-white solid (2.72 g, 28% yield). The solid was used in the next reaction without further purification.

In a N_2-filled glove box, lithium aluminum hydride (1.55 g, 6.0 equiv.) was suspended in anhydrous diethyl ether (80 mL). The mixture was stirred overnight and filtered through a Celite-packed funnel. To the colorless lithium aluminum hydride solution, **2a** (1.97 g, 1.0 equiv.) was added slowly in portions, during which time the reaction solution turned cloudy. The mixture was allowed to stir for **3d** before work-up. The excess lithium aluminum hydride was quenched by sequential addition of deionized water, 10% sodium hydroxide solution, and deionized water. The mixture was diluted with a mixture of 1:1 diethyl ether/water and stirred. The solid was removed by filtration, and the aqueous portion was extracted once again with diethyl ether. The combined organic phase was dried over magnesium sulfate and concentrated. **3a** was purified by vacuum distillation to afford a colorless liquid (0.98 g, 55% yield). B.p. = 75 °C at 85 mTorr. ^{1}H-NMR (500 MHz, $CDCl_3$): 7.39–7.27 (m, 4H), 7.25–7.17 (m, 1H), 3.82 (q, J = 6.8 Hz, 1H), 2.92–2.79 (m, 4H), 2.71 (m, 6H), 2.64–2.53 (m, 2H), 2.34 (s, 6H), 1.35 (d, J = 6.7 Hz, 3H). ^{13}C-NMR (126 MHz, $CDCl_3$): 144.39, 128.12, 128.04, 126.72, 63.74, 57.57, 56.73, 53.15, 46.58, 16.99. HR-ESI-TOF-MS: 262.2279 ($C_{16}H_{28}N_3^+$, $[M+H]^+$; calc. 262.2283).

1-[(2*R*)-3,3-Dimethylbutan-2-yl]-4,7-dimethyl-1,4,7-triazonane (**3b**). This compound can be prepared by the same method as for **3a**. Compound **2b** was prepared from LiBr (6.48 g, 2.0 equiv.), Na_2CO_3 (31.60 g, 8.0 equiv.), bischloroacetamide **1** (9.00 g, 1.0 equiv.), and MeNp–NH_2 (5.45 mL, 1.1 equiv.) in anhydrous acetonitrile (500 mL). Compound **3b** was then prepared from **2b** (8.02 g, 1.0 equiv.) and lithium aluminum hydride (6.00 g, 6.0 equiv.) in anhydrous diethyl ether (200 mL). Overall yield: 1.59 g (18%). Colorless liquid, b.p. = 61 °C at 190 mTorr. ^{1}H-NMR (500 MHz, $CDCl_3$): 3.16 (m, 2H), 2.80–2.71 (m, 4H), 2.59 (m, 2H), 2.47 (m, 2H), 2.40 (m, 2H), 2.33 (s, 6H), 2.25–2.18 (m, 1H), 0.91–0.87 (m, 12H). ^{13}C-NMR (126 MHz, $CDCl_3$): 69.76, 58.24, 56.95, 55.41, 47.01, 35.89, 28.48, 7.67. HR-ESI-TOF-MS: 242.2592 ($C_{14}H_{32}N_3^+$, $[M+H]^+$; calc. 242.2596).

1,4-Di-*tert*-butyl-7-[(1*S*)-1-phenylethyl]-1,4,7-triazonane (**6a**). An oven-dried 200 mL Schlenk flask under N_2 was charged with Na_2CO_3 (4.07 g, 2.5 equiv.), and bischloroacetamide **4** (5.00 g, 1.0 equiv.) in anhydrous DMF (150 mL). To the stirred mixture was added PhEt–NH_2 (2.2 mL, 1.1 equiv.) in one portion. The mixture was heated to 120 °C overnight and cooled to room temperature. The mixture was poured into water (80 mL) and extracted with CH_2Cl_2 (3×70 mL). The combined organic layer was washed with brine (4×80 mL), dried over $MgSO_4$, and concentrated *in vacuo*. The oily crude was triturated with minimal Et_2O, and hexane was added to complete precipitation. The solid was collected by filtration to afford **5a** as an off-white solid (4.01 g, 70% yield). The solid was used in the next reaction without further purification.

Compound **6a** was then prepared by the same method as for **3a** from **5a** (3.00 g, 1.0 equiv.) and lithium aluminum hydride (1.83 g, 6.0 equiv.) in anhydrous diethyl ether (100 mL). Yield: 1.23 g (44%). Colorless liquid, b.p. = 114 °C at 5 mTorr. ^{1}H-NMR (500 MHz, $CDCl_3$): 7.46 (d, J = 7.2 Hz, 2H), 7.35–7.28 (m, 2H), 7.20 (t, J = 7.3 Hz, 1H), 3.74 (q, J = 6.7 Hz, 1H), 2.85–2.56 (m, 12H), 1.33 (d, J = 6.7, 3H), 1.03 (s, 18H). ^{13}C-NMR (126 MHz, $CDCl_3$): 146.29, 127.97, 127.93, 126.26, 62.86, 54.88, 54.10, 53.13, 51.64, 27.14, 17.80. HR-ESI-TOF-MS: 346.3224 ($C_{22}H_{40}N_3^+$, $[M+H]^+$; calc. 346.3222).

1,4-Di-*tert*-butyl-7-[(2*R*)-3,3-dimethylbutan-2-yl]-1,4,7-triazonane (**6b**). This compound can be prepared by the same method as for **6a**. Compound **5b** was prepared from Na_2CO_3 (4.07 g, 2.5 equiv.), bischloroacetamide **4** (5.00 g, 1.0 equiv.), and MeNp–NH_2 (2.25 mL, 1.1 equiv.) in anhydrous DMF (150 mL). Compound **6b** was then prepared from **5b** (2.94 g, 1.0 equiv.) and lithium aluminum hydride (1.92 g, 6.0 equiv.) in anhydrous diethyl ether (100 mL). Overall yield: 2.29 g (46%). Colorless liquid, b.p. = 104 °C at

10 mTorr. ^{1}H-NMR (500 MHz, $CDCl_3$): 3.07–2.93 (m, 2H), 2.87 (m, 2H), 2.65 (m, 4H), 2.54–2.34 (m, 4H), 2.09 (q, J = 6.9 Hz, 1H), 1.02 (s, 18H), 0.93–0.88 (m, 12H). ^{13}C-NMR (126 MHz, $CDCl_3$): 68.35, 56.18, 54.73, 52.13, 50.87, 36.07, 28.68, 27.16, 7.78. HR-ESI-TOF-MS: 326.3524 ($C_{20}H_{44}N_3^+$, $[M+H]^+$; calc. 326.3535).

[(3a)$_2$Ni$_2$(μ-Cl)$_3$](PF$_6$) (**7**). In a 20 mL vial, compound **3a** (50 mg, 1.05 equiv.) and KPF_6 (16.7 mg, 0.50 equiv.) were dissolved in 2 mL MeCN. To the mixture was then added $NiCl_2$(DME) (40 mg, 1.00 equiv.), and the solution immediately turned teal with the formation of white precipitate. The solution was allowed to stir overnight, and the white solid was filtered off. The solution was evaporated to dryness and redissolved in 1,2-difluorobenzene (1.5 mL). To the concentrated solution was added pentane (6 mL) slowly, and the vial was left overnight to allow precipitation. Complex **7** was obtained as a teal solid (76 mg, 94% yield) by filtration. X-ray quality crystals were obtained from slow evaporation of a concentrated MeCN/THF solution at room temperature. Anal. calc. for $C_{32}H_{54}Cl_3N_6Ni_2PF_6$: C 43.54, H 6.18, N 9.08; found: C 43.11, H 6.10, N 9.43. ^{1}H-NMR (500 MHz, CD_3CN): 126.17, 119.99, 41.18, 9.29, 6.79, 5.45, 2.14, 2.09, 2.05, −4.13. ESI-MS: Formate adduct observed [(**3a**)Ni^{II}(HCOO)]$^+$, calculated: 364.1540. Found: 364.1519.

[(3b)NiCl$_2$] (**8**). To a 20 mL vial was added **3b** (108 mg, 1.05 equiv.), $NiCl_2$(DME) (92 mg, 1.00 equiv.), and 2 mL MeCN. The solution was allowed to stir overnight, and 4 mL Et_2O was added. The green precipitate was collected by filtration, washed with 2 mL Et_2O, and dried *in vacuo*. Complex **8** was obtained as a green solid (137 mg, 88% yield). X-ray quality crystals were obtained from slow diffusion of diethyl ether into an acetonitrile solution at −35 °C. Anal. calc. for $C_{14}H_{31}Cl_2N_3Ni$: C 45.29, H 8.36, N 11.13; found: C 45.32, H 8.42, N 11.33. ^{1}H-NMR (500 MHz, CD_3CN): 146.56, 127.78, 116.16, 105.00, 89.68, 70.83, 44.85, 41.09, 39.16, 35.08, 30.85, 21.98, 14.20, 3.65, 2.62, 1.81, −5.39. ESI-MS: Formate adduct observed [(**3b**)Ni^{II}(HCOO)]$^+$, calculated: 344.1853. Found: 344.1834.

[(6a)NiCl](PF$_6$) (**9**). To a 20 mL vial was added **6a** (100 mg, 1.05 equiv.), KPF_6 (51 mg, 0.50 equiv.), 0.5 mL Et_2O, and 2.5 mL MeCN. While stirring, $NiCl_2$(DME) (61 mg, 1.00 equiv.) was added, and the solution slowly turned orange overnight. The white precipitate was removed by filtration. To the orange solution was added 50 mL Et_2O, and the resulting solution was placed in a −35 °C freezer for crystallization. The orange precipitate was collected by filtration, washed with Et_2O, and dried *in vacuo*. **9** was obtained as an orange solid (149 mg, 92% yield). X-ray quality crystals were obtained from slow evaporation of a concentrated MeCN/THF solution at room temperature. Anal. calc. for $C_{22}H_{39}ClN_3NiPF_6{\cdot}0.5CH_3CN$: C 45.60, H 6.83, N 8.32; found: C 45.65, H 6.75, N 8.10%. ^{1}H-NMR (500 MHz, CD_3CN): 11.28, 10.56, 7.44, 5.37, 1.24, 0.94. ESI-MS: Formate adduct observed [(**6a**)Ni^{II}(HCOO)]$^+$, calculated: 448.2479. Found: 448.2469.

[(6b)NiCl](PF$_6$) (**10**). To a 20 mL vial was added **6b** (78 mg, 1.05 equiv.), KPF_6 (44 mg, 0.50 equiv.), 0.5 mL Et_2O, and 2.5 mL MeCN. While stirring, $NiCl_2$(DME) (50 mg, 1.00 equiv.) was added, and the solution slowly turned orange overnight. The white precipitate was removed by filtration. To the orange solution was added 14 mL Et_2O, and the resulting solution was placed in a −35 °C freezer for crystallization. The orange precipitate was collected by filtration, washed with Et_2O, and dried *in vacuo*. Complex **10** was obtained as an orange solid (79 mg, 61% yield). X-ray quality crystals were obtained from slow evaporation of a concentrated MeCN/THF solution at room temperature. Anal. calc. for $C_{20}H_{43}ClN_3NiPF_6$: C 42.45, H 7.73, N 7.53; found: C 42.54, H 7.68, N 7.44. ^{1}H-NMR (500 MHz, CD_3CN): 16.28, 11.03, 7.10, 1.99. ESI-MS: Formate adduct observed [(**6b**)Ni^{II}(HCOO)]$^+$, calculated: 428.2792 Found: 428.2778.

General Procedure for the Kumada Cross-Coupling Reactions

All catalytic reactions were performed as follows, unless otherwise noted. In a N_2-filled glovebox, a 2 M solution of *n*-octyl-MgCl (75 μL, 1.5 equiv., 0.15 mmol) was diluted to 0.5 mL with THF. The stock solution was then slowly added by the syringe pump over 1 h to a solution containing a ligand (12 mol%, 0.012 mmol), $NiCl_2$(DME) (2.2 mg, 10 mol%, 0.01 mmol), 1.25 mL of THF and 0.25 mL of MeCN (50 equiv.), and *n*-heptyl iodide (16.8 μL, 0.1 mmol) at room temperature, premixed for 5 min. After the addition, the solution was stirred for an additional hour, and then it was quenched by the addition of 2 mL of saturated NH_4Cl solution. Dodecane (22.7 μL, 0.1 mmol) was then added as an internal standard. The organic phase in the resulting solution mixture was extracted with 4 mL of ether and subjected to GC-MS analysis.

Supporting Information

The authors have cited additional references within the *Supporting Information*.[27–31] Supporting information for this article is available on the WWW under https://doi.org/10.1002/hlca.202300170. Deposition Number(s) 2296612 (for **10**), 2296613 (for **9**), 2296614 (for **8**), and 2296615 (for **7**) contain(s) the supplementary crystallographic data for this paper. These data are provided free of charge by the joint Cambridge Crystallographic Data Centre and Fachinformationszentrum Karlsruhe Access Structures service.

Author Contribution Statement

C.-H. H. performed the metal complex synthesis and characterization. J. B. C. performed cross-coupling experiments. C.-H. H., J. B. C., and L. M. M. analyzed the data. All authors contributed to the preparation of the manuscript.

Acknowledgements

We thank the National Science Foundation (CHE-2155160 to L.M.M.) and the Taiwan UIUC fellowship (1070055211 A to C.-H.H) and for financial support of this research. We also thank Dr. Toby Woods for help with X-ray crystal structure analysis.

Conflict of Interest

The authors declare no conflicts of interest.

Data Availability Statement

The data that support the findings of this study are available in the *Supporting Information*, or from the corresponding author upon reasonable request.

References

[1] R. Hage, J. E. Iburg, J. Kerschner, J. H. Koek, E. L. M. Lempers, R. J. Martens, U. S. Racherla, S. W. Russel, T. Swarthoff, R. P. van Vliet, J. B. Warnaar, L. van der Wolf, B. Krijnen, 'Efficient manganese catalysts for low-temperature bleaching', *Nature* **1994**, *369*, 637–639.

[2] T. Joshi, M. Kubeil, A. Nsubuga, G. Singh, G. Gasser, H. Stephan, 'Harnessing the Coordination Chemistry of 1,4,7-Triazacyclononane for Biomimicry and Radiopharmaceutical Applications', *ChemPlusChem* **2018**, *83*, 554–564.

[3] H.-J. Cho, T. T. Huynh, B. E. Rogers, L. M. Mirica, 'Design of a multivalent bifunctional chelator for diagnostic ^{64}Cu PET imaging in Alzheimer's disease', *Proc. Natl. Acad. Sci. USA* **2020**, *117*, 30928–30933.

[4] H.-J. Cho, A. K. Sharma, Y. Zhang, M. L. Gross, L. M. Mirica, 'A Multifunctional Chemical Agent as an Attenuator of Amyloid Burden and Neuroinflammation in Alzheimer's Disease', *ACS Chem. Neurosci.* **2020**, *11*, 1471–1481.

[5] L. Sun, H.-J. Cho, S. Sen, A. S. Arango, N. Bandara, Y. Huang, T. T. Huynh, B. E. Rogers, E. Tajkhorshid, L. M. Mirica, 'Amphiphilic Distyrylbenzene Derivatives as Potential Therapeutic and Imaging Agents for the Soluble Amyloid β Oligomers in Alzheimer's Disease', *J. Am. Chem. Soc.* **2021**, *143*, 10462–10476.

[6] Y. Huang, H.-J. Cho, N. Bandara, L. Sun, D. Tran, B. E. Rogers, L. M. Mirica, 'Metal-chelating benzothiazole multifunctional compounds for the modulation and ^{64}Cu PET imaging of Aβ aggregation', *Chem. Sci.* **2020**, *11*, 7789–7799.

[7] Y. Wang, T. T. Huynh, H.-J. Cho, Y.-C. Wang, B. E. Rogers, L. M. Mirica, 'Amyloid β-Binding Bifunctional Chelators with Favorable Lipophilicity for ^{64}Cu PET Imaging in Alzheimer's Disease', *Inorg. Chem.* **2021**, *60*, 12610–12620.

[8] R. Hoerres, H. M. Hennkens, '1,4,7-Triazacyclononane-Based Chelators for the Complexation of [^{186}Re]Re- and [^{99m}Tc]Tc-Tricarbonyl Cores', *Inorg. Chem.* **2023**, doi.org/10.1021/acs.inorgchem.3c01934.

[9] J. R. Khusnutdinova, F. Qu, Y. Zhang, N. P. Rath, L. M. Mirica, 'Formation of the Pd(IV) Complex $[(Me_3tacn)Pd^{IV}Me_3]^+$ through Aerobic Oxidation of $(Me_3tacn)Pd^{II}Me_2$ (Me_3tacn = *N*,*N*′,*N*″-trimethyl-1,4,7-triazacyclononane)', *Organometallics* **2012**, *31*, 4627–4630.

[10] F. Qu, J. R. Khusnutdinova, N. P. Rath, L. M. Mirica, 'Dioxygen activation by an organometallic Pd(II) precursor: formation of a Pd(IV)–OH complex and its C–O bond formation reactivity', *Chem. Commun.* **2014**, *50*, 3036–3039.

[11] M. B. Watson, N. P. Rath, L. M. Mirica, 'Oxidative C–C Bond Formation Reactivity of Organometallic Ni(II), Ni(III), and Ni(IV) Complexes', *J. Am. Chem. Soc.* **2017**, *139*, 35–38.

[12] C.-H. Hu, S.-T. Kim, M.-H. Baik, L. M. Mirica, 'Nickel-Carbon Bond Oxygenation with Green Oxidants via High-Valent Nickel Species', *J. Am. Chem. Soc.* **2023**, *145*, 11161–11172.

[13] M. S. Okamoto, E. K. Barefield, 'Cobalt(III) complexes of cyclic triamine 1,4,7-triazacyclononane and Aminoalcohol Ligands', *Inorg. Chim. Acta* **1976**, *17*, 91–96.

[14] D. H. Peacock, Y. S. Gwan, 'Polyamines Part III. The Preparation of Unsymmetrical Amines of the Types $NHR\text{-}C_2H_4{\cdot}NHC_2H_4NH_2$ and $NH_2C_2H_4NHC_3H_6NH_2$ and the Action of Ammonia on Di-*p*-toluenesulphonylbis-(β-chloroethyl)-ethylenediamine', *J. Chem. Soc.* **1937**, 1468–1471.

[15] H. Koyama, T. Yoshino, 'Syntheses of Some Medium Sized Cyclic Triamines and Their Cobalt(III) Complexes', *Bull. Chem. Soc. Jpn.* **1972**, *45*, 481–484.

[16] J. E. Richman, T. J. Atkins, 'Nitrogen Analogs of Crown Ethers', *J. Am. Chem. Soc.* **1974**, *96*, 2268–2270.

[17] D. A. Valyaev, S. Clair, L. Patrone, M. Abel, L. Porte, O. Chuzel, J.-L. Parrain, 'Grafting a homogeneous transition metal catalyst onto a silicon AFM probe: a promising

strategy for chemically constructive nanolithography', *Chem. Sci.* **2013**, *4*, 2815–2821.
[18] A. Thangavel, M. Wieliczko, J. Bacsa, C. C. Scarborough, '1,4,7-Triazacyclononane Ligands Bearing Tertiary Alkyl Nitrogen Substituents', *Inorg. Chem.* **2013**, *52*, 13282–13287.
[19] T. C. Pickel, G. J. Karahalis, C. T. Buru, J. Bacsa, C. C. Scarborough, 'Synthesis of Previously Inaccessible Derivatives of 1,4,7-*Tri*-R-1,4,7-Triazacyclononane, Including Chiral Examples, and a Rapid Synthesis of the HCl Salts of H_3tacn and H_4dtne', *Eur. J. Org. Chem.* **2018**, 6876–6889.
[20] N. H. Evans, R. Carr, M. Delbianco, R. Pal, D. S. Yufit, D. Parker, 'Complete stereocontrol in the synthesis of macrocyclic lanthanide complexes: direct formation of enantiopure systems for circularly polarised luminescence applications', *Dalton Trans.* **2013**, *42*, 15610–15616.
[21] L. Griego, T. J. Woods, L. M. Mirica, 'A five-coordinate Ni(I) complex supported by 1,4,7-triisopropyl-1,4,7-triazacyclononane', *Chem. Commun.* **2022**, *58*, 7360–7363.
[22] L. Griego, J. B. Chae, L. M. Mirica, 'Triisopropyl-1,4,7-Triazacyclononane, a Goldilocks Ligand for Probing the Role of Ni(III) and Ni(I) Centers in Cross-Coupling Catalysis', *Chem* **2023**, in press.
[23] A. Grenz, S. Ceccarelli, C. Bolm, 'Synthesis and application of novel catalytically active polymers containing 1,4,7-triazacyclononanes', *Chem. Commun.* **2001**, 1726–1727.
[24] M. J. Belousoff, M. B. Duriska, B. Graham, S. R. Batten, B. Moubaraki, K. S. Murray, L. Spiccia, 'Synthesis, X-ray Crystal Structures, Magnetism, and Phosphate Ester Cleavage Properties of Copper(II) Complexes of N-Substituted Derivatives of 1,4,7-Triazacyclononane', *Inorg. Chem.* **2006**, *45*, 3746–3755.
[25] K. E. Krakowiak, J. S. Bradshaw, R. M. Izatt, 'Preparation of Triaza-Crown, Tetraaza-Crown and Peraza-Crown Compounds Containing Aminoalkyl Side Groups or Unsubstituted Ring Nitrogen-Atoms', *J. Org. Chem.* **1990**, *55*, 3364–3368.
[26] U. Bossek, D. Nühlen, E. Bill, T. Glaser, C. Krebs, T. Weyhermüller, K. Wieghardt, M. Lengen, A. X. Trautwein, 'Exchange Coupling in an Isostructural Series of Face-Sharing Bioctahedral Complexes $[LM^{II}(\mu\text{-}X)_3M^{II}L]BPh_4$ (M=Mn, Fe, Co, Ni, Zn; X=Cl, Br; L=1,4,7-Trimethyl-1,4,7-triazacyclononane)', *Inorg. Chem.* **1997**, *36*, 2834–2843.
[27] Bruker, 'APEXIII. Bruker AXS, Inc.', Madison, Wisconsin, USA, 2018.
[28] L. Krause, R. Herbst-Irmer, G. M. Sheldrick, D. Stalke, 'Comparison of silver and molybdenum microfocus X-ray sources for single-crystal structure determination', *J. Appl. Crystallogr.* **2015**, *48*, 3–10.
[29] G. Sheldrick, '*SHELXT* - Integrated space-group and crystal-structure determination', *Acta Crystallogr. Sect. A* **2015**, *71*, 3–8.
[30] G. M. Sheldrick, 'A short history of SHELX', *Acta Crystallogr. Sect. A* **2008**, *64*, 112–122.
[31] G. M. Sheldrick, 'Crystal structure refinement with *SHELXL*', *Acta Crystallogr. Sect. C* **2015**, *71*, 3–8.

Received September 24, 2023
Accepted November 15, 2023

